Analysis of Measured Magnetization and Pull Characteristics

By R. L. PEEK, Jr.

(Manuscript received September 21, 1953)

It is shown in this article that the observed magnetization relations of most ordinary electromagnets conform to simple expressions which can be interpreted as the flux vs. magnetomotive force equations of a reluctance network, analogous to the current-voltage equations of a resistance network. To the extent of such conformity the magnetic circuit constants characterizing the network suffice for the evaluation of the field energy and pull characteristics of the electromagnet. The agreement between the observed magnetization and these simple relations is close in the region of linear magnetization, and is adequate for engineering purposes at higher flux densities, but the extent of agreement in the latter range varies with the type of structure and the location of the magnetic parts which first approach saturation.

Specific analytical and graphical procedures are given for the evaluation of the magnetic circuit constants from both pull and magnetization measurements. These procedures employ relations which give linear plots indicating the degree of conformity of the observed relations to the expressions used to fit them. The relation of the measured constants to those which can be estimated in design[1] is discussed, as is the use and application of the measured constants in development and engineering studies.

1 INTRODUCTION

In the design of telephone relays and similar switching apparatus, the characteristics of the electromagnet which serves as motor element may be distinguished from those of the mechanical system of contact springs and actuating members which it operates. The performance of the electromagnet is characterized statically by the mechanical work done for a given coil energization, and dynamically by the time required to actuate the mechanical load, including in this the inertia of the moving parts.

Both the potential work output of the electromagnet and the energy stored in developing its field can be evaluated from its magnetization

relations. The consequent dependence of the pull and timing characteristics upon the magnetization relations makes the measurement and analysis of the latter fundamental to the understanding of performance and its relation to design.

Procedures are described in this article for the evaluation from measured magnetization relations of a few parameters which suffice for the determination of the pull and of the field energy under given conditions. These parameters, the magnetic circuit constants, characterize the electromagnet to which they apply. They are used as measures of performance in comparing different structures, or in studying the effect of dimensional or material variations in a particular design.

In addition to their significance as parameters summarizing measured magnetization relations, the magnetic circuit constants may be interpreted as the observed values of quantities postulated in the magnetic circuit approximation to static field theory. This approximation is discussed in a companion article,[1] which describes methods of estimating the values of the magnetic circuit constants from the configuration, dimensions, and materials constant of the electromagnet. Comparison of observed and estimated values of these constants has served as a guide in developing these methods of estimation. A complete design methodology is provided by the ability to both estimate and measure the magnetic circuit constants characterizing the performance of electromagnets.

In the experimental evaluation of the magnetic circuit constants described in this article, the basic method is that employing measured magnetization relations. Because of the dependency of the pull upon the magnetization relations, pull measurements may also be used, subject to certain limitations, for the evaluation of the magnetic circuit constants. The article includes description of procedures for doing this.

The notation used in this article conforms to the list that is given on page 257.

2 MAGNETIZATION RELATIONS

The magnetization relations of an electromagnet give the average flux φ linked per turn of the winding as a function of the two determining variables: applied ampere turns NI and armature position x. The relations are usually shown, as in Fig. 1, as a family of curves giving φ versus NI for various values of x. Armature motion is usually rotary, and the choice of the location at which x is measured is a matter of convenience. The curves of Fig. 1 apply to the electromagnet shown in Fig. 2, the AJ (heavy duty) type of wire spring relay described in an article

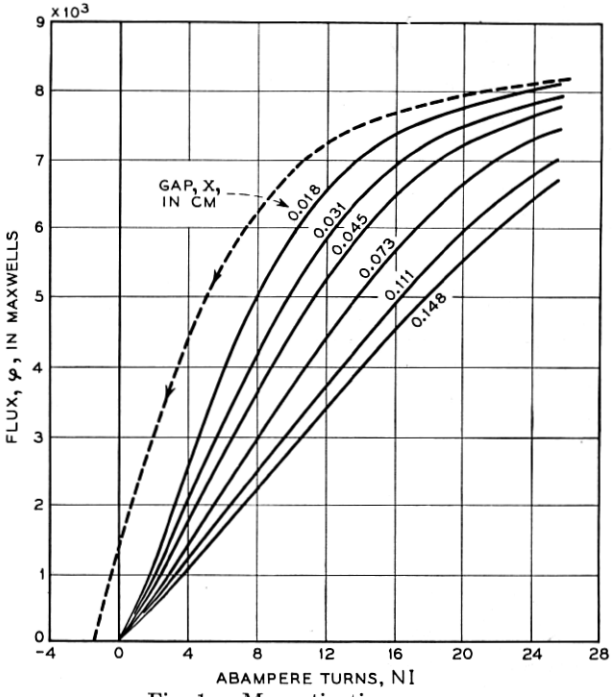

Fig. 1 — Magnetization curves.

by A. C. Keller.[2] In this case it is convenient to measure x at the center line of the actuating card, whose location with respect to the axis of rotation is indicated in Fig. 2.

Apart from interpretation in terms of magnetic theory, any observed point on a magnetization curve represents a measurement of the electrical energy U stored in the coil, as given by the integral

$$\int_0^I ei\,dt,$$

where $e = d(N\varphi)/dt$. It is represented by the area between the magnetization curve and the axis of φ, and is given by:

$$U = \int_0^{\varphi} NI\,d\varphi. \tag{1}$$

This stored field energy may, in principle, be recovered in the decay of the field, except for the portion lost by hysteresis in the material, represented by the area between the increasing and decreasing mag-

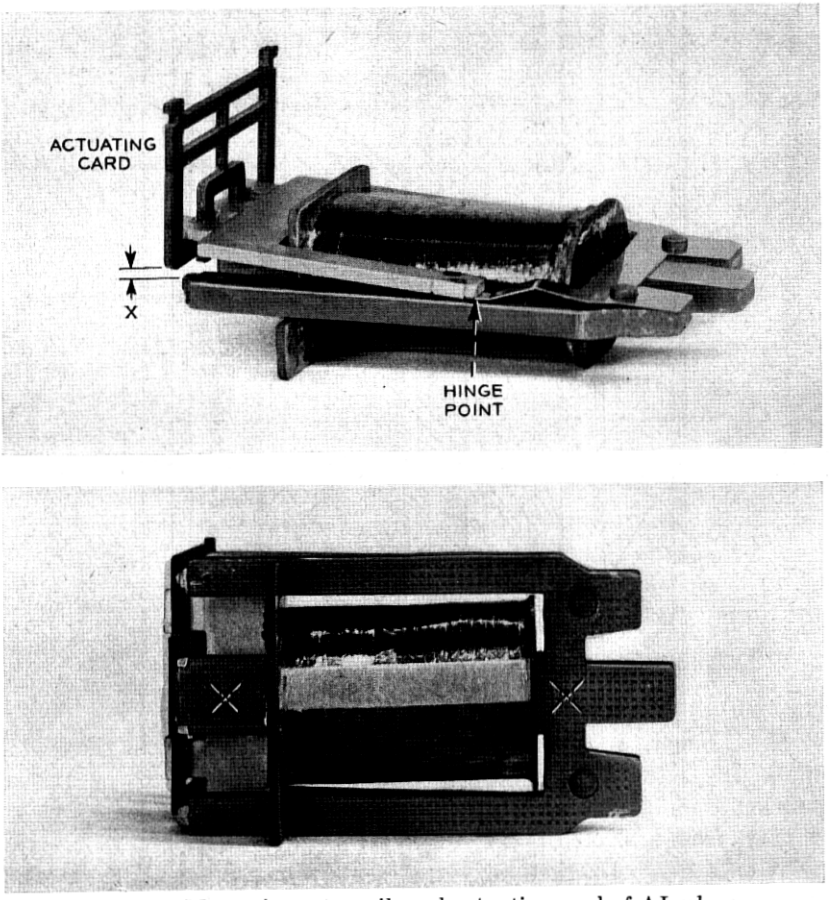

Fig. 2 — Magnetic parts, coil, and actuating card of AJ relay.

netization curves. The dashed curve of Fig. 1 is the decreasing magnetization curve for the same gap as the adjacent magnetization curve.

U is a function of x, and changes as the armature moves. If this motion occurs at a constant value of φ, there is no induced voltage and hence no electrical transfer of energy. A decrease in U must therefore represent mechanical work done on the armature. For a differential change dx in armature position, the mechanical work is Fdx, where F is the pull exerted on the armature. A general expression for F is therefore given by:

$$F = \frac{\partial U}{\partial x}_{(\varphi \text{ constant})} . \tag{2}$$

It follows from these considerations of energy balance that the magnetization relations determine the relations among the electrical input to the coil, the stored energy, and the mechanical output attainable. Hence, any generally applicable and simple expression for the magnetization relations, even if purely empirical, would provide a convenient means for evaluating and describing the performance characteristics.

The expressions given below for the magnetization relations are not purely empirical, but are those obtained as approximate solutions to the magnetic field equations by the magnetic circuit method. When experimentally evaluated, however, their utility in defining the characteristics of the electromagnet to which they apply is independent of this interpretation, and depends only on their conformity to the observed magnetization relations.

It is convenient to formulate the expressions for the magnetization curves in terms of the reluctance $\mathcal{R}$, the ratio $\mathcal{F}/\varphi$, where $\mathcal{F}$ is the magnetomotive force $4\pi NI$. The observations of Fig. 1 are plotted in Fig. 3 in the form of curves giving $\mathcal{R}$ vs. NI for various values of x. A constant value of φ is represented in such a plot by a straight line through the origin. The radial lines used as supplementary co-ordinates are spaced to give a convenient scale for φ.

The reluctance curves of Fig. 3 are similar in character to those applying to most ordinary electromagnets. Each curve has a relatively flat characteristic in the vicinity of a minimum located on a common flux

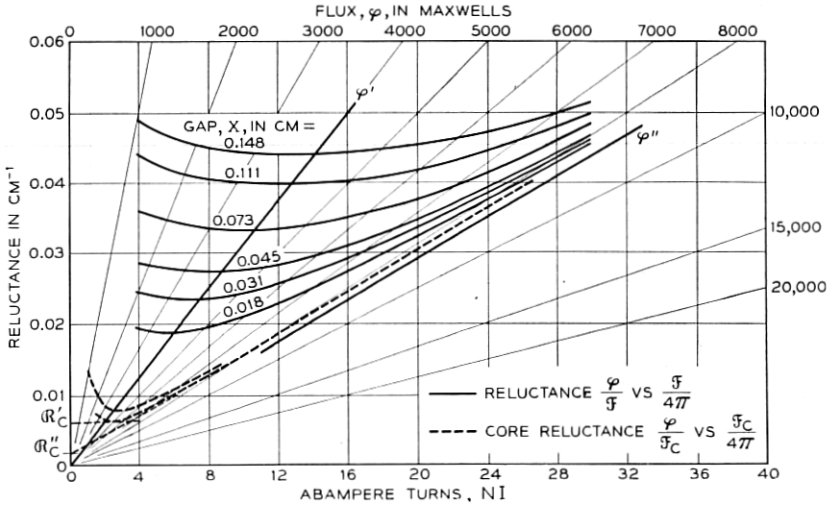

Fig. 3 — Reluctance curves.

line, that marked φ' in the figure. At values of φ above this minimum, the reluctance increases at an increasing rate, indicating an upper limit to the value of φ approached as NI becomes very large. The observed value of φ' may be interpreted as that for which the core density corresponds to maximum permeability, while the indicated upper limit may be interpreted as the saturation flux φ''.

The observations plotted in Figs. 1 and 3 were obtained with the sample initially demagnetized, a convenient reference condition for measurement. In actual use, relays and other electromagnets have been previously operated, and the applicable φ versus $\mathfrak{F}$ relation is that for repeated magnetization. In this case there is little or no increase in reluctance below φ'. For engineering purposes, the reluctance below φ' may be taken as constant at the value observed at φ' in measurements made from an initially demagnetized condition. This assumption is equivalent to taking the φ versus $\mathfrak{F}$ relation as linear up to the "knee" of the curve, the point of tangency with a line through the origin.

It follows that expressions for the magnetization relations may take $\mathfrak{R}$ as a function of x only, independent of φ, in the low density region, $\varphi < \varphi'$, while for $\varphi > \varphi'$, modified expressions must be employed which show $\mathfrak{R}$ increasing with φ, and approaching $\mathfrak{F}/\varphi''$.

Magnetic Circuit Schematics

The reluctance expressions for the magnetization relations can be conveniently defined by the magnetic circuit schematics shown in Figs. 4, 5, and 6. In these the reluctance $\mathfrak{R}$, or $\mathfrak{F}/\varphi$, is represented by a network of component reluctances, analogous to a network of electrical resistances, with flux analogous to current, and magnetic potential analogous to voltage. Thus the reluctance corresponding to Fig. 4 is given by:

$$\mathfrak{R} = \frac{\mathfrak{R}_L\left(\mathfrak{R}_0 + \frac{x}{A}\right)}{\mathfrak{R}_L + \mathfrak{R}_0 + \frac{x}{A}}. \tag{3}$$

The interpretation of the parameters $\mathfrak{R}_0$, $\mathfrak{R}_L$, and A in terms of the magnetic circuit concept is discussed in the companion article cited above.[1] In the analysis of experimental results they are parameters which summarize measurements in which the observed values of $\mathfrak{R}$ conform to (3). From this viewpoint Fig. 4 indicates only that the total flux φ is the sum of a flux φ_L for which the reluctance is constant, and a flux φ_G for which the reluctance varies directly with x.

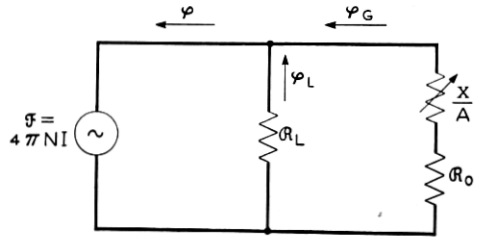

Fig. 4 — Equivalent magnetic circuit.

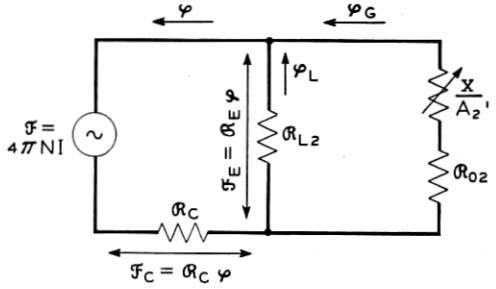

Fig. 5 — Magnetic circuit for core saturation.

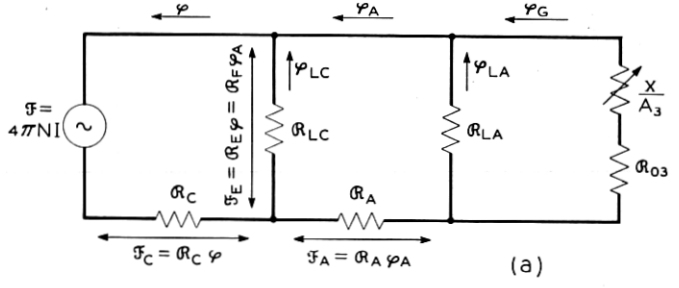

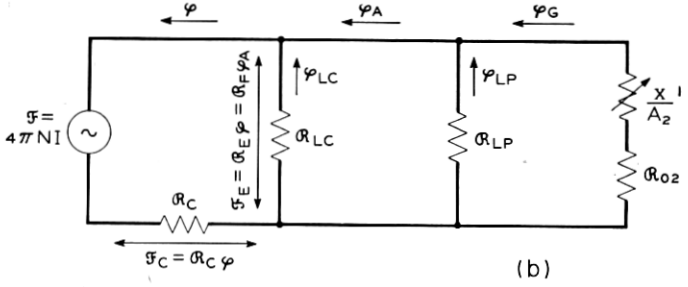

Fig. 6 — Magnetic circuit for armature saturation.

In Fig. 4, $\mathcal{R}_0$, $\mathcal{R}_L$, and A are constants, so that $\mathcal{R}$ is a function of x only, independent of φ. Equation (3) can then apply only to the low density region, $\varphi < \varphi'$. For most ordinary electromagnets, the magnetization relations for $\varphi < \varphi'$ conform to (3), and hence to the schematic of Fig. 4.

For $\varphi > \varphi'$, the expression for $\mathcal{R}$ must provide for the variation with φ. It usually suffices to use an expression in which the only term varying with φ is that corresponding to the path in which saturation first occurs. The most common case is that in which saturation first occurs in the core. The reluctance can then be taken as conforming to the schematic of Fig. 5, in which $\mathcal{R}_{02}$, $\mathcal{R}_{L2}$ and A_2 are constants, and $\mathcal{R}_C$ is a function of φ only. The total reluctance is given by:

$$\mathcal{R} = \mathcal{R}_C + \mathcal{R}_E, \tag{4}$$

where:

$$\mathcal{R}_E = \frac{\mathcal{R}_{L2}\left(\mathcal{R}_{02} + \dfrac{x}{A_2}\right)}{\mathcal{R}_{L2} + \mathcal{R}_{02} + \dfrac{x}{A_2}}. \tag{5}$$

If the variation with φ is taken as conforming to the empirical Frohlich-Kennelly equation,[6] $\mathcal{R}_C$ is given by:

$$\mathcal{R}_C = \mathcal{R}_C'' \frac{\varphi''}{\varphi'' - \varphi} = \mathcal{R}_C' \frac{\varphi'' - \varphi'}{\varphi'' - \varphi}, \tag{6}$$

where φ'' is the saturation flux and φ' is the flux for maximum permeability or minimum reluctance $\mathcal{R}_C'$. If these assumptions apply, the minimum values of $\mathcal{R}$ for all values of x must lie on φ', as for the results of Fig. 3. This common minimum is thus evidence that the core is controlling with respect to the variation with φ, and that (4) and (6) are applicable. As (6) applies only for $\varphi > \varphi'$, $\mathcal{R}_C'$ is the value of $\mathcal{R}_C$ not only at $\varphi = \varphi'$, but throughout the low density region $\varphi < \varphi'$. In the alternative form given by (6), $\mathcal{R}_C''$ is defined by this equation, and represents merely the intercept of a plot of $\mathcal{R}_C$ extended below the region to which (6) applies.

In some electromagnets saturation occurs in the armature rather than in the core. This is the case, for example, in high speed relays in which the armature section is minimized to reduce its mass. In such cases, the reluctance conforms to the schematic of Fig. 6(a), in which $\mathcal{R}_A$ represents the reluctance of the armature, which varies with φ_A. As the ratio φ_A/φ

then varies with x, the minimum values of $\mathcal{R}$ do not lie on a common value of φ in this case.

In Fig. 6(a), $\mathcal{R}_A$ may be taken as given by an expression of the same form as (6), with φ' and φ'' replaced by the minimum and saturation values of φ_A, and $\mathcal{R}_C'$ replaced by the minimum value of $\mathcal{R}_A$. $\mathcal{R}_C$ may be taken either as given by (6), or as a constant if the variation in $\mathcal{R}_A$ is dominant. The other parameters of Fig. 6(a) are constants. The expression for $\mathcal{R}$ applying to Fig. 6(a) may be obtained in the same manner as those given for the circuits of Figs. 4 and 5.

The magnetic circuits of Figs. 5 and 6 are called "design" circuits, because their constants may be estimated from the dimensions and material constants of the design, as discussed in the companion article.[1] Estimates of the corresponding values of the equivalent magnetic circuit constants of Fig. 4 are obtained from these design constant estimates by the equivalence equations given below.

Conditions of Equivalence

Whatever magnetic circuit is taken as applying, the component reluctances are independent of φ in the low density region, $\varphi < \varphi'$, and are therefore constants except for the gap reluctance. If this varies directly as x, as assumed in the schematics shown, the reluctance for any circuit reduces to an expression of the form of (3), applying to the circuit of Fig. 4. As shown in the companion article,[1] the reluctance of the circuit of Fig. 5 when $\mathcal{R}_C$ is constant is given by (3) when the parameters of this equation are given by:

$$\begin{aligned} \mathcal{R}_L &= \mathcal{R}_{L2} + \mathcal{R}_C , \\ A &= \frac{A_2}{p^2} , \\ \mathcal{R}_0 &= p^2\mathcal{R}_{02} + p\mathcal{R}_C , \end{aligned} \tag{7}$$

where:

$$p = 1 + \frac{\mathcal{R}_C}{\mathcal{R}_{L2}} .$$

These relations are the conditions of equivalence, for which the reluctances of Figs. 4 and 5 are identical for all values of x. With them, the reluctance given by (4) can be reduced to the simpler form of (3) when $\mathcal{R}_C$ is a constant, as throughout the low density region.

Similar relations apply to the magnetic circuit of Fig. 6(a). In particu-

lar, when $\mathcal{R}_A$ is a constant, the reluctance $\mathcal{R}_F$, or $\mathcal{F}_E/\varphi_A$, represented by the series parallel path of φ_A in Fig. 6(a), may be represented by the simple parallel path of φ_A in Fig. 6(b). By analogy with equations (7) the constants applying are related by:

$$\mathcal{R}_{LP} = \mathcal{R}_{LA} + \mathcal{R}_A ,$$

$$A_2 = \frac{A_3}{p^2} , \tag{7A}$$

$$\mathcal{R}_{02} = p^2\mathcal{R}_{03} + p\mathcal{R}_A ,$$

where

$$p = 1 + \frac{\mathcal{R}_A}{\mathcal{R}_{LA}} .$$

The circuit of Fig. 6(b) is identical with that of Fig. 5 with $1/\mathcal{R}_{L2}$ equal to the sum of $1/\mathcal{R}_{LC}$ and $1/\mathcal{R}_{LP}$. Thus the circuit of Fig. 6(a) may be reduced to that of Fig. 5 when $\mathcal{R}_A$ is constant. The resulting circuit may be reduced in turn to the equivalent circuit of Fig. 4 when $\mathcal{R}_C$ is constant. Thus the equivalent circuit may be used to represent all cases in the low density region, where the component reluctances are independent of φ, provided the gap reluctance varies linearly with x.

3 ANALYSIS OF MAGNETIZATION MEASUREMENTS

In analysing the observed magnetization relations, it is convenient to treat the low density and high density relations in separate and successive steps. For the former, the analysis is based on the equivalent magnetic circuit of Fig. 4.

EVALUATION OF EQUIVALENT MAGNETIC CIRCUIT CONSTANTS

For a given value of x, the total reluctance in the low density region is taken as constant at the minimum value $\mathcal{R}'(x)$ observed in measurements made from the demagnetized condition. If the observations are plotted as reluctance curves, as in Fig. 3, these values of $\mathcal{R}'(x)$ may be read directly. When the recording fluxmeter[3] is used, $\mathcal{R}'(x)$ can be obtained from the φ versus $\mathcal{F}$ curve as the slope $\mathcal{F}/\varphi$ of the line through the origin tangent to the curve. The reciprocals $P(x)$ of the values of $\mathcal{R}'(x)$ thus evaluated may be plotted against x. Values of $P(x)$ corresponding to the minimum reluctance values of Fig. 3 are plotted in this way in Fig. 7. The origin of x is taken as for a gap of 0.025 cm., corresponding to the operated position of the actuating card for maximum stop pin height.

Values of x measured from this origin are termed travel, as distinguished from gap values, which are measured from the position of iron to iron contact.

If the relation between $\mathfrak{R}'(x)$ and x conforms to (3), the values of $P(x)$ must conform to:

$$P(x) = \frac{1}{\mathfrak{R}_L} + \frac{A}{A\mathfrak{R}_0 + x}. \tag{8}$$

Then if x_C is a central reference value of x, and $P(x_C)$ the corresponding value of $P(x)$, the expression for $P(x_C) - P(x)$ given by (8) may be written in the form:

$$\frac{x - x_C}{P(x_C) - P(x)} = A\left(\mathfrak{R}_0 + \frac{x_C}{A}\right)^2 + \left(\mathfrak{R}_0 + \frac{x_C}{A}\right)(x - x_C). \tag{9}$$

Thus conformity with (3) requires the ratio given by (9) to vary linearly with x. This ratio is plotted against $x - x_C$ in Fig. 7, referred to the upper and right hand scales. The values of this ratio are sensitive to deviations in the values of x and $P(x)$ near x_C, and minor variations from linearity are to be expected here. Allowing for this, the results agree with (9), and the relation between $\mathfrak{R}'(x)$ and x therefore conforms to (3).

From (9), the slope and intercept of the linear plot may be interpreted as indicated in Fig. 7. Then A may be evaluated by dividing the intercept

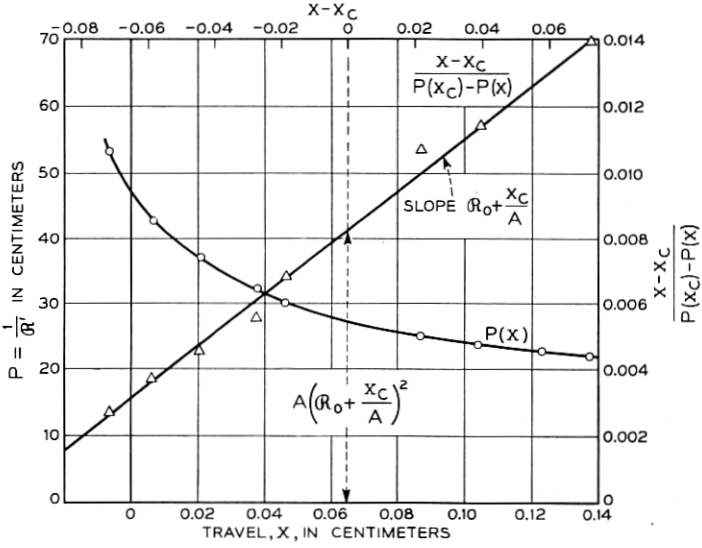

Fig. 7 — Evaluation of equivalent circuit constants.

value by the square of the slope value, and the latter then serves to evaluate $\mathcal{R}_0$ by subtracting x_c/A. On substituting these values of $\mathcal{R}_0$ and A in (8) at $x = x_c$, $\mathcal{R}_L$ may be evaluated. For the case plotted in Fig. 7, the values thus obtained are:

$$\mathcal{R}_0 : 0.0300 \text{ cm}^{-1}$$

$$A : 1.34 \text{ cm}^2$$

$$\mathcal{R}_L : 0.0690 \text{ cm}^{-1}$$

These values of the equivalent circuit constants, substituted in (3), suffice to accurately characterize the magnetization relations and thus the electromagnet's performance through the low density region.

Evaluation of High Density Relations

For cases of core saturation, the high density relations may be analysed in terms of the magnetic circuit of Fig. 5. The corresponding reluctance is given by (4), in which $\mathcal{R}_C = \mathcal{R}_C'$ for $\varphi = \varphi'$. If $\mathcal{R}_C'$ can be determined, the three parameters determining $\mathcal{R}_E$ in (5) may be evaluated by the equivalence equations (7). To determine $\mathcal{R}_C$ through the high density region from (6) requires evaluation of $\mathcal{R}_C'$, φ', and φ''. Thus the analysis of the high density relations requires evaluation of these three quantities in addition to the three parameters of the equivalent circuit evaluated above.

A method for evaluating $\mathcal{R}_C'$, φ', and φ'' directly from the magnetization curves is described subsequently, following a description of a preferred method which requires additional measurements. These measurements are determinations of the drop $\mathcal{R}_C\varphi$ in magnetic potential through the core, and are conveniently made with the magnetomotive force gauge developed by W. B. Ellwood.[4]

Magnetomotive Force Measurements

The Ellwood mmf gauge measures the difference in magnetic potential between the outer ends of the two reeds of a dry reed switch, as determined by the coil current required to open the switch. The end of one reed is used as a probe, which is brought into contact with the magnetic structure being measured. The end of the other reed, at a distance of about 5 cm from the probe, then lies on a relatively distant surface surrounding the structure: this surface is substantially at the same potential for any position of the gauge. Then the difference between two such measurements made at different points on the magnetic structure measures the difference in magnetic potential between them.

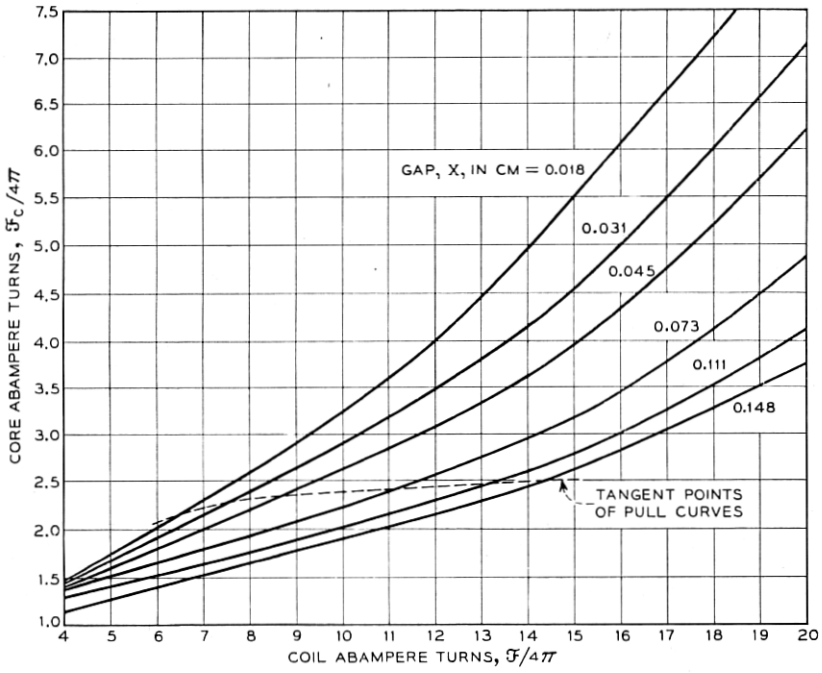

Fig. 8 — Relation of core potential drop to applied magnetomotive force.

To the extent that the physical structure may be identified with the corresponding magnetic circuit element, the drop in magnetic potential in the core may be identified with $\mathfrak{R}_C\varphi$ in Fig. 5. Assuming this identification to apply, magnetic probe measurements may be made at the two ends of the core, as at the points marked X in Fig. 2. The potential drop observed in these measurements is the magnetic potential $\mathfrak{F}_E$ applied to the external magnetic circuit. $\mathfrak{F}_E$ is equal to the applied magnetomotive force $\mathfrak{F}$(or $4\pi NI$) less the potential drop $\mathfrak{F}_C = \mathfrak{R}_C\varphi$ in the core. Thus $\mathfrak{F}_C = \mathfrak{F} - \mathfrak{F}_E$. Values of $\mathfrak{F}_C/(4\pi)$ thus determined for the relay of Fig. 2 are shown plotted against $\mathfrak{F}/(4\pi)$ for various values of x in Fig. 8. These curves are substantially linear in the low density region: their upward concavity at higher values of $\mathfrak{F}$ is evidence that saturation first occurs in the core.

Evaluation of Core Relucatance Constants

The magnetization curves of Fig. 1 and the core magnetomotive force curves of Fig. 8 were obtained with the same model. For given values of $\mathfrak{F}$ and x there can be read from these two figures corresponding values of

φ and $\mathfrak{F}_C$, giving the corresponding values of core reluctance $\mathfrak{R}_C = \mathfrak{F}_C/\varphi$. Such values of $\mathfrak{F}_C$ have been determined for two values of x (the smallest and largest included in these figures), and are shown plotted against $\mathfrak{F}_C/(4\pi)$ in the dashed curves included in Fig. 3. Values of $\mathfrak{R}_C$ for intermediate values of x are intermediate between these two curves, whose similarity supports the assumption of Fig. 5 and equation (4) that $\mathfrak{R}_C$ is substantially independent of x.

For $\varphi > \varphi'$ the plot of $\mathfrak{R}_C$ versus $\mathfrak{F}_C$ is substantially linear. In this it conforms to (6) which, by substitution of $\mathfrak{F}_C/\mathfrak{R}_C$ for φ, may be written in the form:

$$\mathfrak{R}_C = \mathfrak{R}_C'' + \frac{\mathfrak{F}_C}{\varphi''} = \left(1 - \frac{\varphi'}{\varphi''}\right)\mathfrak{R}_C' + \frac{\mathfrak{F}_C}{\varphi''}. \tag{10}$$

Thus φ'' may be evaluated from the slope of the plot of $\mathfrak{R}_C$ versus $\mathfrak{F}_C$, and $\mathfrak{R}_C''$ from the intercept of the dotted line extension, as indicated in Fig. 3. The observed relation deviates from (10) in the vicinity of φ', and the linear relation conforming to (10) does not intersect $\mathfrak{R}_C'$ at φ', but at some higher value of φ. Thus (6) more nearly represents the observed relation if φ' is taken as this higher value, rather than at the flux for minimum $\mathfrak{R}$ previously taken as φ' and marked at such in Fig. 3. The error in using this latter value of φ' in (6), however, is minor, and of little significance in engineering estimates.

Alternative Method of Determining Core Reluctance Constants

When magnetomotive force measurements are not made, the core reluctance constants can be determined directly from the magnetization curves as follows:

As can be seen in Fig. 3, the line representing φ'' can be directly identified as the apparent asymptote of the reluctance curves: specifically by determining the flux line parallel to the tangent to the upper portion of the lowest reluctance curve. As φ' is the value of φ at which the reluctance curves have their common minima, φ' and φ'' can be readily evaluated, and only $\mathfrak{R}_C'$ remains to be determined.

On substituting $\mathfrak{F}/\mathfrak{R}$ for φ in (6), and substituting this expression for $\mathfrak{R}_C$ in (4) the resulting equation can be solved to give:

$$\mathfrak{R} = \frac{1}{2}\left(\mathfrak{R}_E + \mathfrak{R}_C'' + \frac{\mathfrak{F}}{\varphi''} + \sqrt{\left(\mathfrak{R}_E + \mathfrak{R}_C'' - \frac{\mathfrak{F}}{\varphi''}\right)^2 + 4\mathfrak{R}_C''\frac{\mathfrak{F}}{\varphi''}}\right).$$

Let $\mathfrak{R}''$ be the particular value of $\mathfrak{R}$ for which

$$\mathfrak{F} = \mathfrak{R}'\varphi'' = (\mathfrak{R}_C' + \mathfrak{R}_E)\varphi''.$$

As both $\mathfrak{R}_c'/\mathfrak{R}'$ and $\mathfrak{R}_c''/\mathfrak{R}'$ are small, substitution of $\mathfrak{F} = \mathfrak{R}'\varphi''$ in the preceding expression gives as an approximation:

$$\mathfrak{R}'' = \mathfrak{R}' + \sqrt{\mathfrak{R}_c''\mathfrak{R}'},$$

from which:

$$\mathfrak{R}_c'' = \frac{(\mathfrak{R}'' - \mathfrak{R}')^2}{\mathfrak{R}'}. \tag{11}$$

Thus, as indicated in Fig. 9, the value of $\mathfrak{R}'$ may be read from any one of the reluctance curves, and the corresponding value of $\varphi''\mathfrak{R}'$ computed. The value of $\mathfrak{R}$ corresponding to $\mathfrak{F} = \mathfrak{R}'\varphi''$ is read from the curve, and taken as $\mathfrak{R}''$. The values of $\mathfrak{R}''$ and $\mathfrak{R}'$ are then substituted in (11) to determine $\mathfrak{R}_c''$. This procedure may be followed for all the reluctance curves, and a mean value of $\mathfrak{R}_c''$ computed. $\mathfrak{R}_c'$ is then taken as

$$\varphi''\mathfrak{R}_c''/(\varphi'' - \varphi').$$

Evaluation of External Reluctance Constants

The procedures described above provide for the determination (a) of the equivalent constants of Fig. 4, (b) of the minimum value $\mathfrak{R}_c'$ of $\mathfrak{R}_c$ in Fig. 5. The remaining constants of Fig. 5 can then be computed by means of the equivalence equations (7). Table I lists, for the measurements of Figs. 1 and 8, the values of the equivalent constants deter-

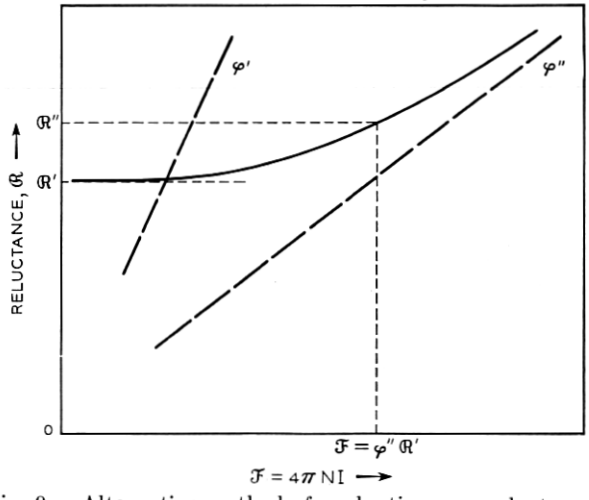

Fig. 9 — Alternative method of evaluating core reluctance.

TABLE I — EVALUATION OF MAGNETIC CIRCUIT CONSTANTS

Equivalent Values (Fig.4)	Design Values (Fig. 5)
From Fig. 7 $\mathcal{R}_0$: 0.0300 cm^{-1} A: 1.34 cm^2 $\mathcal{R}_L$: 0.0690 cm^{-1}	From Fig. 3 $\mathcal{R}_C'$: 0.0070 cm^{-1} From equations (7) $\mathcal{R}_{02}$: 0.0181 cm^{-1} A_2 : 1.66 cm^2 $\mathcal{R}_{L2}$: 0.0620 cm^{-1}

mined in Fig. 7, and the value of $\mathcal{R}_C'$ determined in Fig. 3. These values have been substituted in equations (7) to determine the component terms of $\mathcal{R}_E$.

The constants applying to Fig. 5 are of interest primarily for comparison with the values computed from the design, as discussed in the companion article.[1] While formally required to evaluate the high density magnetization relations, they are not explicitly required in estimating the high density pull, as is shown in a later section.

The reluctance $\mathcal{R}_E$ of equations (4) and (5) can be evaluated experimentally through the full range of the magnetization measurements when the magnetomotive force measurements are available. Thus Figs. 1 and 3 can be used to determine values of φ and $\mathcal{F}_E$ (or $\mathcal{F} - \mathcal{F}_C$) for corresponding values of $\mathcal{F}$ and x. In this way there have been obtained the curves of $\mathcal{R}_E$ plotted against $\mathcal{F}_E$ for various values of x in Fig. 10. These curves are included here merely to illustrate the approximate validity of (4), in which $\mathcal{R}_E$ is taken as independent of φ. The departures from this condition are minor except for the smaller gaps at high values

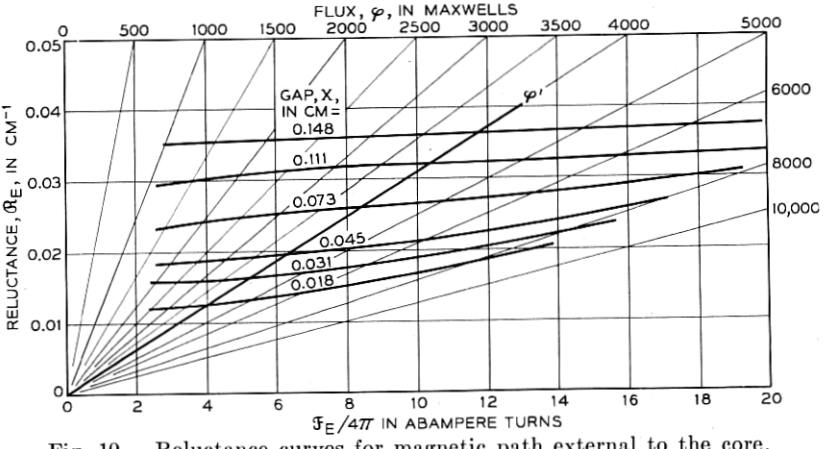

Fig. 10 — Reluctance curves for magnetic path external to the core.

of φ. Here the increase in flux density in the iron parts external to the core results in a significant increase in $\mathcal{R}_E$ as φ increases. By comparison with the plot of $\mathcal{R}_C$ included in Fig. 1, however, this increase in $\mathcal{R}_E$ is minor, and does not affect the fact that the limiting reluctance is $\mathcal{F}/\varphi''$, where φ'' is the saturation flux of the core.

It may be noted in passing that the values of $\mathcal{R}_E$ lying on φ' must conform to (5). As this is of the same form as (3), these values of $\mathcal{R}_E$ may be used to evaluate the component terms of (5) by the procedure applied to the values of $\mathcal{R}'$ in Fig. 7. As the same data are employed, the values of $\mathcal{R}_{02}$, $\mathcal{R}_{L2}$, and A_2 thus determined agree with those computed by means of equations (7) within the accuracy of the computations.

Case of Armature Saturation

The analysis of the low density relations is, of course, independent of where saturation occurs, and involves merely the determination of the equivalent magnetic circuit constants by the procedure described above. In the high density region, however, the quantities appearing in Fig. 6(a) must be evaluated when armature saturation occurs. This requires measurements not only of $\mathcal{F}$ and φ, but also of $\mathcal{F}_E$ and φ_A.

$\mathcal{F}_E$ is given by the Ellwood mmf gauge measurements previously described. To measure φ_A requires the use of a search coil wound on the armature, located over the region of maximum density. For twin return path structures, such as the relay of Fig. 2, twin search coils must be used, connected to measure the total armature flux. If the variation of $\mathcal{R}_A$ with φ_A is to be determined directly, additional mmf gauge measurements must be made of the potential drop $\mathcal{R}_A\varphi_A$ through the armature.

With φ_A determined as a function of $\mathcal{F}_E$ for various values of x, the reluctance $\mathcal{R}_F$, or $\mathcal{F}_E/\varphi_A$ may be analysed by the procedure described above for the analysis of the reluctance $\mathcal{R}$ or $\mathcal{F}/\varphi$. The curves of $\mathcal{R}_F$ versus $\mathcal{F}_E$ have minima $\mathcal{R}'_F$ at φ'_A. The reciprocals of these values of $\mathcal{R}'_F$ are plotted and analysed as in Fig. 7 to evaluate the equivalent constants $\mathcal{R}_{LP}$, $\mathcal{R}_{02}$, and A_2 of Fig. 6(b). The constants $\mathcal{R}'_A$, φ'_A, and φ''_A characterizing the relation between $\mathcal{R}_A$ and φ_A are determined either from mmf gauge measurements or by the method of Fig. 9. Then the constants $\mathcal{R}_{LA}$, $\mathcal{R}_{03}$, and A_3 of Fig. 6(a) can be evaluated by means of the equivalence equations (7A).

To complete the determination of the quantities appearing in Fig. 6(a), $\mathcal{R}_{LC}$ is evaluated as the ratio $\mathcal{F}_E/(\varphi - \varphi_A)$, while $\mathcal{R}_C$, which may either be constant or conform to (6), is evaluated from the relation between φ and $\mathcal{F}_C$.

4 PULL RELATIONS

As shown in Section 2, the pull F can be determined from the field energy U by means of equation (2). If the gap reluctance varies linearly with x, this equation reduces to:

$$F = \frac{\varphi_G^2}{8\pi A}, \tag{12}$$

as shown in the companion article.[1] Equation (12) is Maxwell's law for the pull between parallel plane surfaces of area A. As used here, $1/A$ has the more general sense of the coefficient of x in a linear expression for the gap reluctance. This equation is therefore applicable to all the cases previously discussed, with A, of course, taken as A_2 or A_3 for the relations applying to Figs. 5 and 6. As with the magnetization relations, it is convenient to give separate consideration to the pull at low densities and that at high densities.

Pull for Linear Magnetization

At low densities, where the magnetization relations are approximately linear, the reluctance conforms to the equivalent magnetic circuit of Fig. 4. In this case, φ_G is given by $\mathfrak{F}/(\mathfrak{R}_0 + x/A)$, and equation (12) becomes:

$$F = \frac{\mathfrak{F}^2}{8\pi A\left(\mathfrak{R}_0 + \frac{x}{A}\right)^2},$$

which may be written in the more familiar form:

$$F = \frac{2\pi(NI)^2}{A\left(\mathfrak{R}_0 + \frac{x}{A}\right)^2}. \tag{13}$$

For conformity with (13) the pull for a given value of x should vary as $(NI)^2$, giving a linear plot with a slope of two when plotted against NI on logarithmic paper. Fig. 11 shows pull measurements of the relay of Fig. 2 plotted in this way. The dashed lines tangent to the curves have a slope of two, and conform in this respect to (13). It is convenient to denote the pull indicated by these dashed lines as F'. Near and below the point of tengency the actual pull F differs little from F'. The pull, like the magnetization, is measured under the condition of initial demagnetization, which gives lower magnetization, and hence less pull, than normally applies in actual use when the magnet has been previously

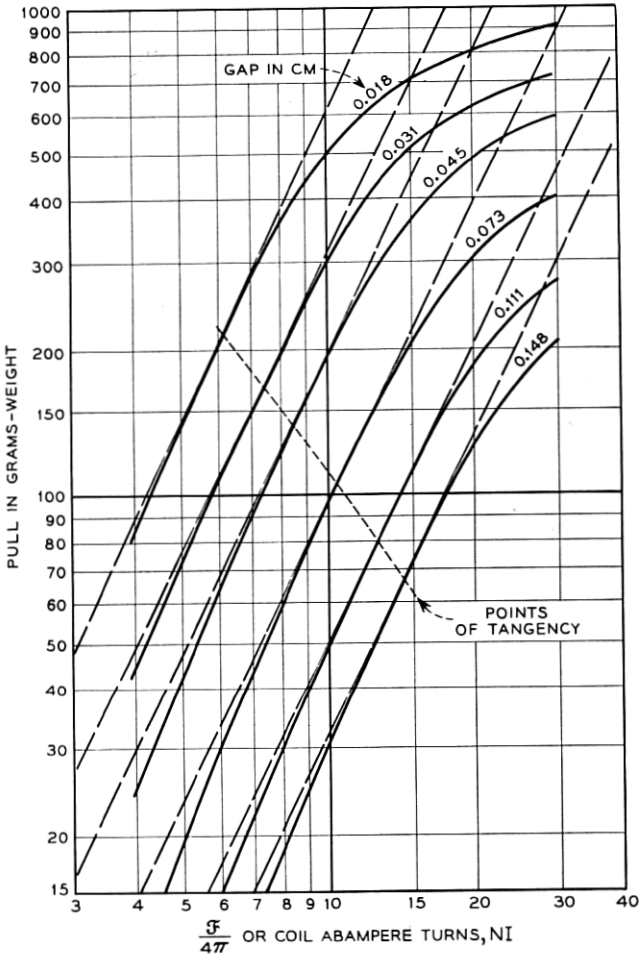

Fig. 11 — Pull curves.

operated. Hence F' satisfactorily represents the pull applying in practice through the low density region. In the high density region, the pull falls off as the result of incipient saturation, and the ratio F'/F increases as $\mathfrak{F}$ (or $4\pi NI$) is increased.

High Density Pull — Core Saturation

It is convenient to express the high density pull in terms of the ratio F'/F, where F is the actual pull, and F' the indicated pull conforming to (13) for the same value of $\mathfrak{F}$ (or $4\pi NI$). As F'/F is unity at low densi-

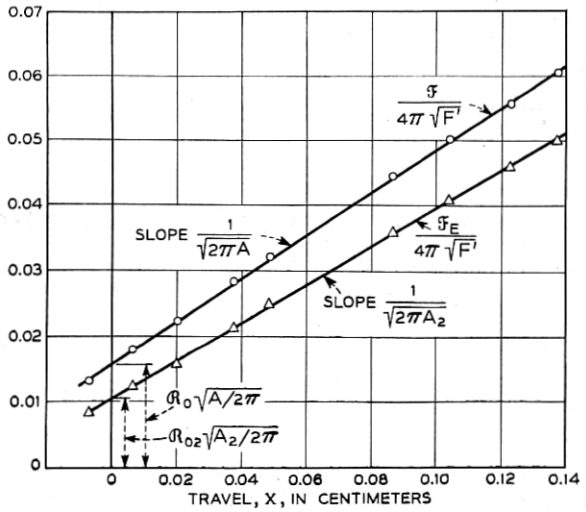

Fig. 12 — Evaluation of magnetic circuit constants from pull data.

Evaluation of Equivalent Magnetic Circuit Constants

The low density pull is given approximately by equation (13), to which the dashed F' lines of Fig. 11 conform. These lines coincide with the actual pull curves at the points of tengency, which must correspond to the minimum reluctance values. Taking F as F', (13) may be written in the form:

$$\frac{\mathfrak{F}}{4\pi\sqrt{F'}} = \mathcal{R}_0\sqrt{\frac{A}{2\pi}} + \frac{x}{\sqrt{2\pi A}}. \tag{18}$$

Values of NI/F' have been determined for the dashed lines of Fig. 11, and are plotted against x in Fig. 12 — the plot marked $\mathfrak{F}/(4\pi\sqrt{F'})$. In agreement with (18) these points determine a straight line. The slope and intercept have been used to determine the values of $\mathcal{R}_0$ and A listed under "Pull Results" in Table II.

As the reluctance $\mathcal{R}_E$ in the circuit of Fig. 5 is identical in form with the reluctance $\mathcal{R}$ of Fig. 4, the pull for Fig. 5 is given by an expression similar to (13), with $\mathfrak{F}$, $\mathcal{R}_0$, and A replaced by $\mathfrak{F}_E$, $\mathcal{R}_{02}$, and A_2, respectively. As the two circuits are equivalent at the points of minimum reluctance and the corresponding points of tangency for the pull curves, the pull at these points is the same for the two cases. Thus if the ratio of $\mathfrak{F}_E$ to $\mathfrak{F}$ is determined at the points of tangency, a plot of $\mathfrak{F}_E/(4\pi\sqrt{F'})$ against x should conform to:

$$\frac{\mathfrak{F}_E}{4\pi\sqrt{F'}} = \mathcal{R}_{02}\sqrt{\frac{A_2}{2}} + \frac{x}{\sqrt{2\pi A_2}}. \tag{19}$$

TABLE II — EVALUATION OF MAGNETIC CIRCUIT CONSTANTS

From Pull Results	From Magnetization Results
$\mathcal{R}_0$: 0.0319 cm^{-1}	0.0300 cm^{-1}
A : 1.46 cm^2	1.34 cm^2
$\mathcal{R}_{02}$: 0.0188 cm^{-1}	0.0181 cm^{-1}
A_2 : 1.85 cm^2	1.66 cm^2
$\mathcal{R}_L$: 0.0630 cm^{-1}	0.0690 cm^{-1}
$\mathcal{R}_{L2}$: 0.0560 cm^{-1}	0.0620 cm^{-1}
$\mathcal{R}_C'$: 0.0072 cm^{-1}	0.0070 cm^{-1}

The points of tangency are indicated on the pull curves of Fig. 11. These values of $\mathfrak{F}$ have been marked on the corresponding curves of Fig. 8, from which can be determined the corresponding values of $\mathfrak{F}_C$, and thus of $\mathfrak{F}_E$. It may be noted in passing that these values of $\mathfrak{F}_C$ are all similar, corresponding to a mean level of about 24 ampere turns, or 30 gilberts. The magnetization results gave values of 4,000 maxwells for φ' (Fig. 3) and of 0.007 cm^{-1} for $\mathcal{R}_C'$ (Table I), giving a value of 28 gilberts for the product. This agrees with the value of $\mathfrak{F}_C$ at the tangent points of the pull curves, showing that these points coincide with the points of minimum reluctance ($\varphi = \varphi'$).

Taking the ratio of $\mathfrak{F}_E$ to $\mathfrak{F}$ as read from the curves of Fig. 8 at the indicated tangent points, the values of $\mathfrak{F}/(4\pi\sqrt{F'})$ in Fig. 12 have been multiplied by the corresponding values of $\mathfrak{F}_E/\mathfrak{F}$, giving the points indicated by triangles in this figure. These conform to a straight line relation, in agreement with (19). The slope and intercept of this linear plot have been used to determine the values of $\mathcal{R}_{02}$ and A_2 listed under "Pull Results" in Table II.

The four quantities determined from the two plots of Fig. 12 appear in the three independent equivalence equations (7), and these three equations may therefore be used to determine the other three quantities: $\mathcal{R}_L$, $\mathcal{R}_{L2}$, and $\mathcal{R}_C'$. The resulting values of these latter quantities are listed under "Pull Results" in Table II. For comparison, the table inincludes the corresponding values of these quantities obtained from the magnetization measurements, and given previously in Table I. The agreement between the results derived from these different kinds of measurements indicates the validity of the analysis described here.

High Density Pull

As previously noted, it is convenient to express the pull F in the high density region in terms of the ratio F'/F, where F' is the pull computed from (13) for the value of $\mathfrak{F}$ applying. F'/F is readily evaluated from a logarithmic plot of the observed pull versus $\mathfrak{F}$, as illustrated by Fig. 11.

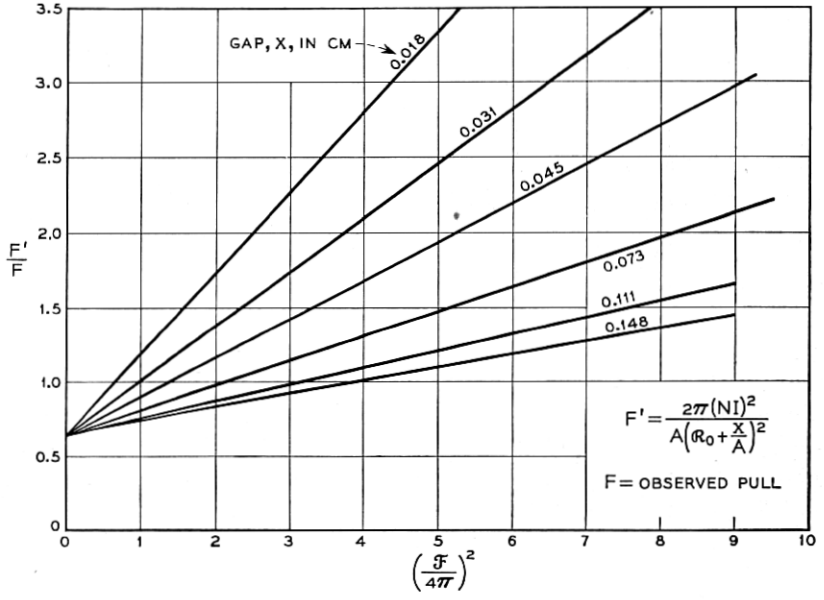

Fig. 13 — Pull characteristics for approaching saturation.

The dashed tangent lines give values of F', so corresponding values of F' and F can be read for various values of $\mathcal{F}$. Values of F'/F for the results of Fig. 11 have been thus determined, and are plotted in Fig. 13 against $(\mathcal{F}/4\pi)^2$ for the values of x applying to the individual curves of Fig. 11.

The values of F'/F thus plotted determine a family of straight lines having a common intercept at the origin of $\mathcal{F}^2$. In this respect these results are representative of the pull characteristics of electromagnets when plotted in this way. As an empirical fact, apart from any analysis, this linearity provides a useful method of plotting pull observations in the high density region, as it facilitates interpolation and the detection of inconsistent observations.

The observed linearity in the relation between F'/F and $\mathcal{F}^2$ conforms to the relations postulated in (15) and (17), of which the former should apply for core saturation. If (15) applies, the common intercept of 0.65 at $\mathcal{F}^2 = 0$ in Fig. 13 should equal $1 - (\varphi'/\varphi'')^2$, indicating a value for φ'/φ'' of 0.59. To determine if the relation fully conforms to (15), the relation between the slopes of the lines and the corresponding values of x must be compared with that indicated by this equation.

Let y^2 be the observed slope of the plot of F'/F versus $\mathcal{F}^2$ for a particu-

lar value of x. If the relation conforms to (15), $y = 1/(\mathcal{R}'\varphi'')$, where $\mathcal{R}'$ is given by (3). Writing C_L for the ratio $(\mathcal{R}_L + \mathcal{R}_0)/\mathcal{R}_0$, and u for the ratio $x/(A\mathcal{R}_0)$,

$$\mathcal{R}' = \frac{1 + u}{C_L + u}\,\mathcal{R}_L ,$$

and hence the values of y should conform to the equation:

$$y(1 + u) = \frac{C_L + u}{\mathcal{R}_L\varphi''} . \tag{20}$$

Using the values of A and $\mathcal{R}_0$ determined from the pull results in Fig. 12 and tabulated in Table II, values of u have been determined for the values of x applying in Fig. 13, and the corresponding values of y have been determined from the slopes of the corresponding lines. The values of $y(1 + u)$ thus determined are shown plotted against u in Fig. 14. The

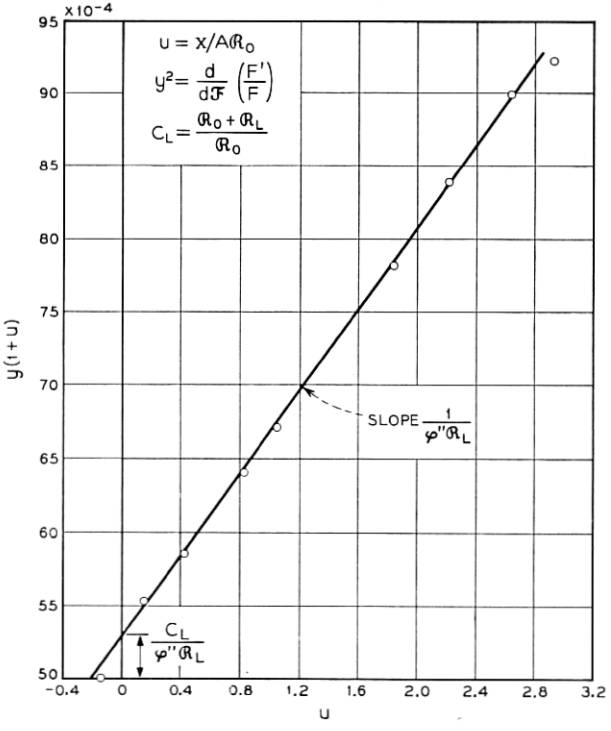

Fig. 14 — Evaluation of saturation flux φ'' and leakage reluctance $\mathcal{R}_L$ from pull characteristics.

TABLE III — EVALUATION OF MAGNETIC CIRCUIT CONSTANTS

From Pull Measurements	From Magnetization Measurements
Figs. 13 & 14:	Fig. 3:
φ': 4,700 maxwells	φ': 4,000 maxwells
φ'': 8,000 maxwells	φ'': 8,500 maxwells
$\mathcal{R}_L$: 0.091 cm^{-1}	
Fig. 12:	Fig. 7:
A: 1.46 cm^2	A: 1.34 cm^2
$\mathcal{R}_0$: 0.0319 cm^{-1}	$\mathcal{R}_0$: 0.0300 cm^{-1}
$\mathcal{R}_L$: 0.063 cm^{-1}	$\mathcal{R}_L$: 0.069 cm^{-1}

resulting plot is linear, in agreement with (20), showing the observed relation between F'/F and $\mathfrak{F}^2$ to conform fully to (15).

The expressions for the slope and intercept given by (20) are indicated in Fig. 14. From the values of the slope and intercept given by the plot, C_L may be evaluated, giving $\mathcal{R}_L$, as $\mathcal{R}_0$ is known. With $\mathcal{R}_L$ thus evaluated, φ'' may be determined from the value of the slope. The values of $\mathcal{R}_L$ and φ'' thus determined from results of Fig. 14 are listed in Table III, together with the value of φ' given by the ratio φ'/φ'' determined from the common intercept in Fig. 13. Included in this table under "Pull Results" are the values of A, $\mathcal{R}_0$, and $\mathcal{R}_L$ determined from the low density data and previously tabulated in Table II. Values of the same quantities as determined from the magnetization measurements are included for comparison.

For both pull and magnetization analysis, empirical relations have been assumed in (6) and (15) for the variation of $\mathcal{R}$ with φ, agreeing with each other and the known conditions only at their upper and lower limits. In view of this, the agreement in the values of φ' and φ'' between the pull and magnetization results is good, and the deviation in the value of $\mathcal{R}_L$ found in Fig. 14 from the other values of this quantity is not surprising.

High Density Pull for Armature Saturation

The low density pull for armature saturation may be analysed as in the case of core saturation. The pull data may be plotted against $\mathfrak{F}$ on logarithmic paper as in Fig. 11, and the tangents of slope two giving F' drawn, as in this figure. The values of $\mathfrak{F}/\sqrt{F'}$ may be plotted as in Fig. 12 to determine A and $\mathcal{R}_0$, and A_2 and $\mathcal{R}_{02}$ also evaluated if $\mathfrak{F}_E$ has been determined from magnetomotive force gauge measurements. As before, the remaining magnetic circuit constants of Figs. 4 and 5 may be de-

termined: the latter in this case are those corresponding to the equivalent schematic of Fig. 6(b).

For the high density pull, values of F'/F may be determined and plotted against $\mathfrak{F}$ as before. The resulting plot is similar to Fig. 13 in showing linear relations for each value of x, radiating from a common intercept. For the presentation of pull results, therefore, this method of plotting is applicable for both core and armature saturation, and for the case where saturation is approached concurrently in both.

When the slopes y^2 are determined, however, and $y(1 + u)$ plotted against u as in Fig. 14, a straight line is not usually obtained unless saturation is confined to the core. The observed relation for armature saturation is usually a curve which is concave upward, and approaches the horizontal at small values of u (travel x small). This result can be interpreted from the expression (17) for F'/F in the case of saturation confined to the armature. The corresponding expression for y is $1/(\mathcal{R}'_F\varphi''_A)$. It was shown above that in this case $\mathcal{R}'_F$ is approximately equal to $\mathcal{R}_0 + x/A$ or $\mathcal{R}_0(1 + u)$. The corresponding expression for $y(1 + u)$ is therefore the constant term $(1/(\mathcal{R}_0\varphi''_A)$. Thus for saturation confined to the armature, the plot of $y(1 + u)$ versus u is simply a horizontal line, from whose value φ''_A can be determined. In the more usual case of concurrent saturation, this relation is approached at small values of u, where φ_A/φ is relatively large, while at larger values of u, where φ_A/φ is smaller, the relation approaches that for core saturation.

6 DISCUSSION

The procedures for the analysis of pull and magnetization measurements described in this article are primarily intended for the evaluation of the magnetic circuit constants in development studies. They also have some related applications, and the choice of procedure varies with the application and with the measurements available. The following discussion of the applications of this analysis indicates the most convenient procedures for each case.

Presentation of Pull Measurements

Pull measurements are used not only for the guidance of development studies, but as engineering data in the application of relays and other electromagnets. A convenient form of presentation is that used in Fig. 11, where the pull is plotted against ampere turns on logarithmic paper. In preparing such data, interpolation of the measurements and the

recognition of inconsistent observations is facilitated by a supplementary plot of F'/F versus $\mathfrak{F}^2$ (or $(NI)^2$) as in Fig. 13.

Estimation of Pull

Estimates of pull are made in preliminary development either from estimates of the magnetic circuit constants, computed from the dimensions as discussed in the companion article,[1] or from magnetization measurements. The low density pull is given by (13), requiring only the equivalent circuit constants A and $\mathfrak{R}_0$ for its evaluation, and is represented by the F' lines of slope two in a logarithmic plot of F versus NI. Estimates of the high density pull may be prepared as linear plots of F'/F versus $(NI)^2$. As these conform (for core saturation) to (15) they require estimates of φ', φ'', and of $\mathfrak{R}'$, as given by (3).

Estimates of pull may also be required in preparing pull data for engineering use, with respect to the changes in pull associated with dimensional and other variations in a commercial product. Such estimates may be obtained by estimating the effect of the variations on the magnetic circuit constants fitting the observed pull, and computing the pull for the changed constants in the manner described in the preceding paragraph.

Evaluation of Equivalent Magnetic Circuit Constants

The equivalent magnetic circuit constants, which define the field energy and the pull characteristics through the low density range, largely suffice for the prediction of performance. This is illustrated by the use of these constants in the analysis of capability relations in one companion article[1] and in the dynamic relations presented in another.[5]

These constants are most readily and accurately evaluated from magnetization data by the procedure illustrated in Fig. 7 and the associated computations. A check on the values of A and $\mathfrak{R}_0$ is provided by analysing pull data by the procedure illustrated in Fig. 12. When only pull data are available, A and $\mathfrak{R}_0$ can be determined in this way, but the determination of $\mathfrak{R}_L$ requires the measurement of $\mathfrak{F}_E$ by the Ellwood mmf gauge. With $\mathfrak{F}_E$ known, the pull results suffice for the determination not only of $\mathfrak{R}_L$, but of the design circuit constants of Fig. 5 (provided saturation is confined to the core).

Evaluation of the Magnetic Design Circuit Constants

The magnetic design circuit constants are required only for comparison with estimated values, in development studies of the effect on the

performance of the configuration, dimensions and materials of the electromagnet. They are most readily and accurately determined from coil magnetization measurements. It is convenient to use Ellwood mmf gauge measurements to determine the core reluctance, but these may be omitted and the method of Fig. 9 employed, provided saturation is confined to the core. Subject to this same limitation, the design constants may be evaluated from the pull measurements if these are supplemented with mmf gauge measurements.

For armature saturation, the magnetic design circuit constants can only be evaluated from magnetization measurements, which must include armature search coil as well as coil flux determinations, and be supplemented by mmf gauge measurements.

Limits of Application

The validity and usefulness of the procedures described here rest on the agreement of measured quantities with the relations used to analyse them. As all the relations used lead to linear plots, the extent of agreement in any specific case is apparent from the plot obtained. So far as the presentation of pull results is concerned, this is the only question of validity involved.

The relations found for the magnetization results are used to estimate the field energy and the pull. To the extent the magnetization results relate to the flux linkages of the coil, the conclusions drawn from relations fitting those results are valid. This follows from the energy balance considerations discussed in Section 2. The supplementary measurements, such as those with the mmf gauge or an armature search coil, are in principle only convenient means for determining the relations to which the coil magnetization conforms. The relations found by these means are only valid to the extent of such agreement.

The conformity of magnetization relations to the expressions used here, corresponding to the magnetic circuit schematics, is closest for electromagnets in which the reluctance of the iron parts is small compared with that of the joints and air gaps. This condition is satisfied for most ordinary relays and similar electromagnets in the low density range, where the expressions given here most closely apply. The expressions used for the high density range do not give as close agreement, but provide a satisfactory basis for engineering analysis, particularly when saturation is confined to the core. The treatment is less satisfactory for structures that deviate from these conditions, such as those with armature saturation, or those with long cores of small cross section, where the

iron reluctance is a major component through the full range of operation.

ACKNOWLEDGMENT

The procedures described in this article incorporate contributions proposed or developed by H. N. Wagar, M. A. Logan, Mrs. K. R. Randall, and others.

REFERENCES

1. R. L. Peek, Jr., and H. N. Wagar, Magnetic Design of Relays, page 23 of this issue.
2. A. C. Keller, New General Purpose Relay, B.S.T.J., **31**, p. 1023, Nov., 1952.
3. H. N. Wagar, Relay Measuring Equipment, page 3 of this issue.
4. W. B. Ellwood, A New Magnetomotive Force Gauge, Rev. Sci. Instr., **17**, p. 109, 1946.
5. Estimation and Control of the Operate Time of Relays: Part I — Theory, R. L. Peek, Jr., page 109 of this issue. Part II — Applications, M. A. Logan, page 144 of this issue.
6. Kennelly, Trans. A.I.E.E., **8**, p. 485, 1891.